

# Differences in moment redistribution in concrete beams prestressed with bonded and unbonded tendons

Katarzyna Mossor

**T**he redistribution of bending moments occurs as a result of a change in stiffness or the appearance of plastic hinges or both at the same time. In reinforced and prestressed concrete beams, the change in stiffness may be a result of cross-section cracking. Taking moment redistribution into account in the calculation of the ultimate limit state may lead to a more economical and efficient design. Moreover, the failure load depends on the extent of moment redistribution before failure. If the required rotation is greater than the available rotation, the beam will fail before reaching the plastic collapse. That is partial redistribution, whereas full redistribution accompanies the development of a plastic collapse mechanism. *Eurocode 2: Design of Concrete Structures*<sup>1</sup> recommends an elastic structural analysis with a limited possibility of redistribution (that is, plastic analysis used only for checking the ultimate limit state). The degree of redistribution  $\delta_i$  is defined as:

$$\delta_i = \frac{M_{i,red}}{M_{i,el}}$$

where

$M_{i,red}$  = bending moment in cross section  $i$  after redistribution

$M_{i,el}$  = bending moment in section  $i$  before redistribution, resulting from the analysis in the elastic range

$i$  = the section identifier

■ Experimental testing was conducted to determine the coefficient of moment redistribution in prestressed concrete beams.

■ Twelve beams were tested for this study, including six continuous beams with either bonded or unbonded tendons and six simply supported beams with either bonded or unbonded tendons. An innovative hybrid approach was used to manufacture the beams, which consisted of a combination of steel elements and a prestressed concrete element.

This paper describes experimental tests to define a more precise method for determining the coefficient of moment redistribution in prestressed concrete beams. The author analyzed beams prestressed with either bonded or unbonded tendons.

## Previous research on the redistribution of bending moments

The phenomena related to the redistribution of bending moments in continuous reinforced and prestressed concrete beams have been studied and described by many authors.<sup>2-6</sup> The research confirms that the amount of reinforcement and its arrangement significantly affect the redistribution of bending moments. The parameters influencing the degree of redistribution are the stiffness of the critical sections, the geometry of the cross section, the type of load, concrete properties, and the occurrence of secondary moments. Pisanty and Regan<sup>7</sup> have suggested that the redistribution of bending moments should be considered in both the ultimate limit state and the serviceability limit state. Li et al.<sup>8</sup> presented an extensive review of research on the redistribution of bending moments in continuous reinforced concrete beams. Based on this review, they proposed the division of redistribution into two stages:

- redistribution in the elastic range, which occurs as a result of concrete cracking
- redistribution in the plastic range, which occurs after yielding of the tension reinforcement when plastic rotation occurs

Leung et al.,<sup>9</sup> Lou et al.,<sup>10</sup> and Zhou and Zheng<sup>11</sup> have examined interesting problems related to moment redistribution in prestressed concrete beams. Leung and colleagues<sup>9</sup> evaluated the influence of the degree of redistribution of bending moments on the load-bearing capacity of prestressed elements. Their paper presents the results of a parametric analysis, performed with the finite element method, of the influence of the degree of redistribution of bending moments on the load capacity of the element and the length of the conventional plastic hinge. With up to 25% redistribution of moments, a 15% reduction in the load capacity of the elements was observed in the case of support sections with low deformability. Moreover, Leung showed that the length of the equivalent plastic hinge has a significant influence on the reduction of the load-bearing capacity of the element, especially for beams with highly deformable support zones. For elements with little deformation over the supports, the influence of the plastic hinge length on the load capacity is insignificant.

Zhou and Zheng<sup>11</sup> analyzed the redistribution of bending moments in beams prestressed using unbonded tendons. Their research confirmed the key influence of the degree of reinforcement on the degree of redistribution of bending moments. The authors proposed empirical formulas for determining the degree of redistribution of bending moments

and for estimating the length of the equivalent plastic hinge in beams prestressed using unbonded tendons.

Based on numerical calculations, Lou et al.<sup>10</sup> performed a critical analysis of the influence of the position of the neutral axis on the redistribution of bending moments for two-span beams stressed externally with carbon-fiber-reinforced polymer tendons. In this analysis, the authors paid particular attention to stiffness differences between the sections in the middle of the span and the section above the central support. The differences in stiffness resulted from the different amounts of reinforcement in these sections. The authors concluded that changes in stiffness differences lead to fundamental changes in the redistribution of bending moments. They also demonstrated that the position of the neutral axis in cross sections should not be the basic criterion for estimating the degree of redistribution.

In a nonlinear analysis of prestressed concrete continuous beams, Campbell and Kodur<sup>12</sup> concluded that the tested finite element model adequately predicts the behavior of a continuous beam over the entire range of loading up to failure. The investigators noted important differences between beams where redistribution of moment is complete at failure and beams where redistribution of moment is incomplete at failure.

The described research on the redistribution of bending moments in prestressed structures and the lack of clear conclusions suggests that further research in this area is necessary.

## Experimental tests

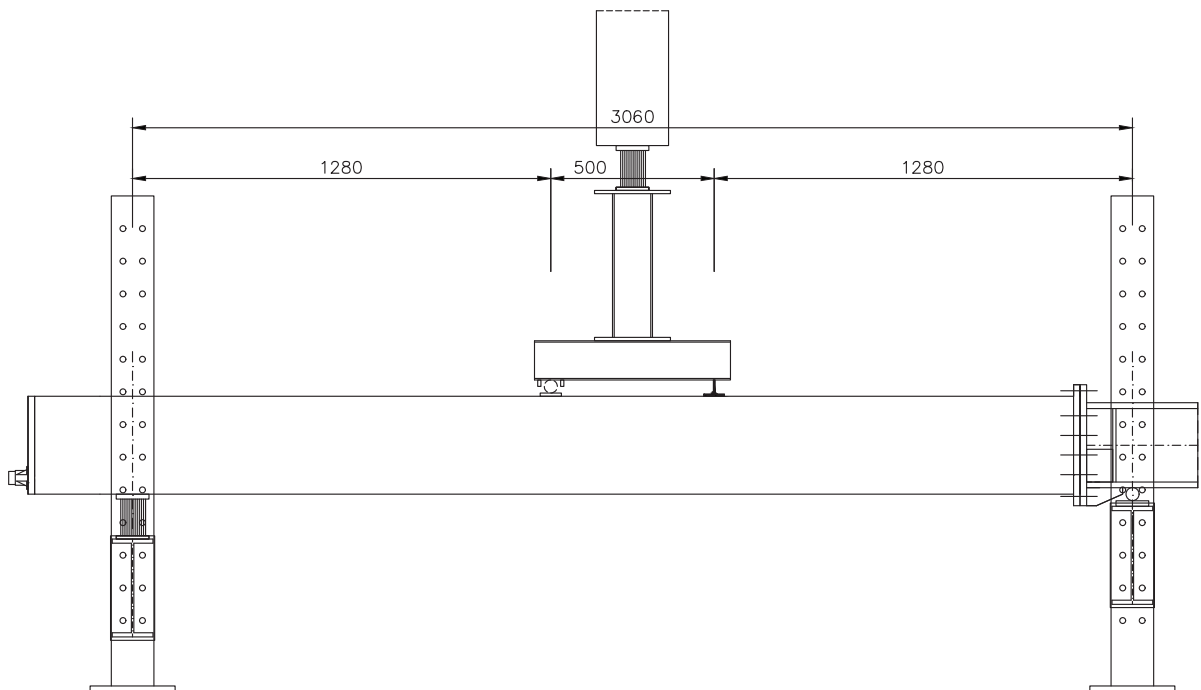
A total of 12 beams were produced and tested for this study. This included six continuous beams with either bonded or unbonded tendons and six simply supported beams with either bonded or unbonded tendons.

Six continuous, two-span beams with spans of 3000 and 4000 mm (118.11 and 157.48 in.) were tested (**Fig. 1**). The beams consisted of a concrete part with a total length of 318 cm (125.197 in.) and a steel part with a total length of 418 cm (164.567 in.). On both sides, the concrete part ended with 20 mm (0.787 in.) thick plates. The cross section of the concrete part was 300 × 300 mm (11.811 × 11.811 in.). The steel part was made of a 260 mm (10.236 in.) I-section. The concrete part was prestressed with tendons made of a single strand. Of the six continuous test beams, three beams were prestressed with bonded tendons and three beams with unbonded tendons. The concrete and steel parts of the beam were connected with a butt joint with 13 bolts.

An innovative research method using a hybrid structure of beams—that is, a combination of a steel element and a prestressed concrete element—was proposed. In the tests, the changes in stiffness occurred in the part made of prestressed concrete, whereas the redistribution of bending moments was estimated on the basis of strain measurements in the steel part. The steel part remained in the elastic field throughout the entire



General View



Longitudinal section

**Figure 1.** Concrete-steel beam used in testing. Note: All dimensions in millimeters. 1 mm = 0.0394 in.

tests. Strain measurements made in a steel element can be more precisely interpreted than measurements in a concrete one due to the constant stiffness and linear-elastic behavior of the steel element in the range of the applied loads. An additional benefit of using this hybrid approach was that the steel part could be used multiple times, with only the concrete part being destroyed each time. The concrete part made contact with the steel part in the area of the zero bending moment, calculated in the range of elastic behavior of the noncracked concrete beam.

Six simply supported beams were also tested. In these beams, the concrete and steel parts were 3180 and 340 mm (125.197 and 13.386 in.) in length, respectively. The other parameters were identical to those in the continuous beams. In the simply supported beams, the axial distance between the support points was assumed to be 3060 mm (120.472 in.) because that distance corresponded to the distance between the zero points of the bending moment in the continuous beam in the range of elastic behavior. Results from the simply supported beams were used to determine the load-bearing capacity limit of the cross section, which was the basis for further analyses.

## Prestressing and test program

The concrete part was stressed by a single strand (with an area of prestressing strand  $A_p$  of 140 mm<sup>2</sup> [0.217in.<sup>2</sup>]). The strand was placed in the cable duct and anchored on both sides using elements from the supplier of the prestressing system. For the beams prestressed with a bonded tendon, the cable duct was grouted after prestressing. In the unbonded tendons, the cable duct was left empty. Prestressing was performed on one side with a prestressing jack, which was also equipped with a hydraulic system to reduce the immediate loss of prestressing force due to anchorage slip. The beams were prestressed with a force of approximately 45 kN (10.1 kip). This force was determined on the basis of the condition that in the middle of the span under the action of the self-weight and the prestressing force, the tensile stresses in the upper fibers reach a value close to zero. Moreover, with this value of prestressing force, the tensile stresses did not exceed the tensile strength of the concrete in the support zones. The amount of time-dependent losses at the time of the research was estimated to be 5 kN (1.1 kip).

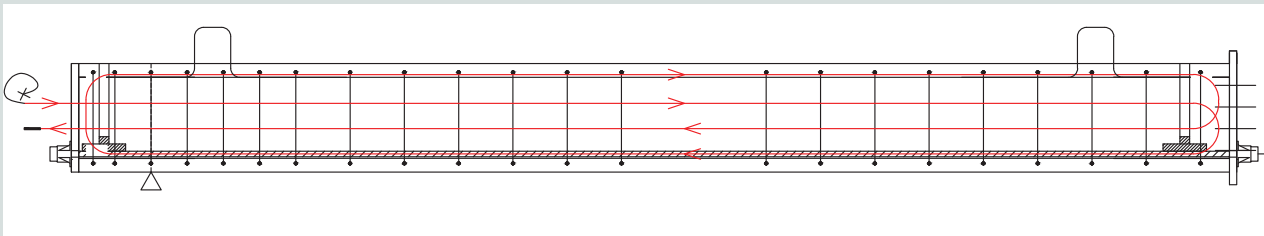


**Figure 2.** Arrangement of the distributed fiber-optic sensors in the longitudinal section.

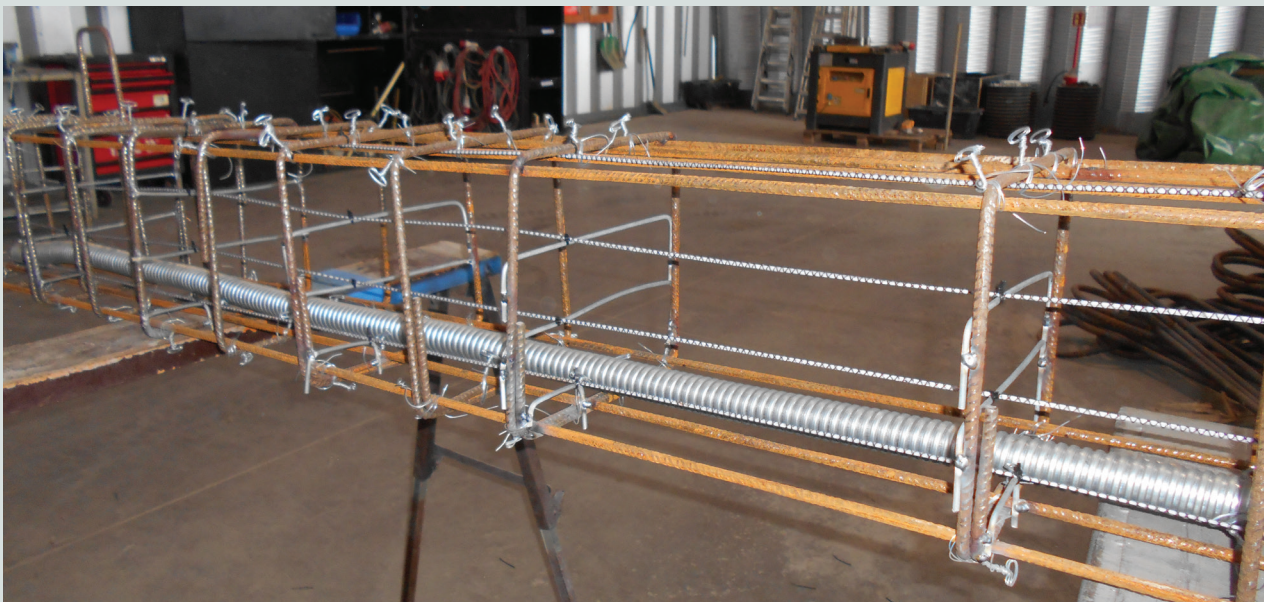


**Figure 3.** Installation of the distributed fiber-optic sensors.

During the tests, the beams were loaded with the actuator via the traverse to achieve pure bending in the middle of the concrete parts of the beams. In the first stage, a force equal to 10 to 20 kN (2.2 to 4.5 kip) was applied with a complete unloading after each value. After completing the first phase of testing, the second fundamental phase of the tests began. The beams were loaded with a force increasing systematically every 10 kN until they were destroyed. The force was increased after stabilizing the deflections under a given load.

## Measurements

In the beams, distributed fiber-optic sensors were used to measure strain. This technique allows the strain to be geo-

metrically measured continuously along the entire length of a single telecommunications optical fiber.<sup>13</sup> The tests were performed with the use of a composite distributed fiber-optic sensor and an optical backscatter reflectometer that has a resolution of strain measurement of  $\pm 1 \mu\epsilon$ . Optical fibers intended for concrete were protected from mechanical damage with special coatings. In each of the 12 concrete beams, one continuous fiber-optic sensor was placed at four different cross-section heights (Fig. 2 and 3). The optical fiber was permanently attached to the reinforcement before concrete was placed. The nonstandard arrangement of the fiber-optic sensors at four cross-section heights allowed for the analysis of changes in the position of the neutral axis.

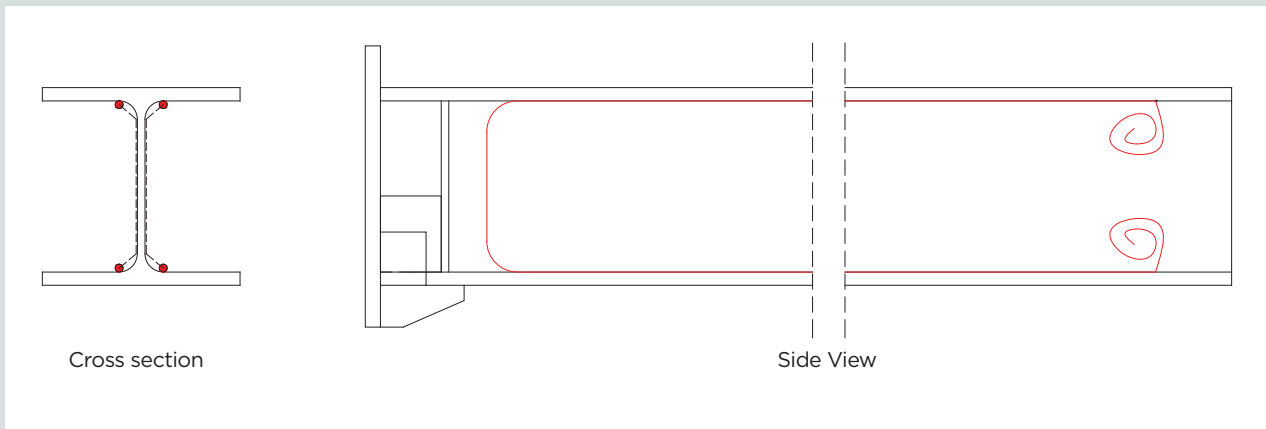


**Figure 4.** Arrangement of the distributed fiber-optic sensors on the steel portion of concrete-steel beam.



**Figure 5.** Simply supported beam with bonded tendons (beam 4) at failure.

In the steel part of the continuous beams, a fiber-optic sensor without protective coatings was used (Fig. 4). The fiber-optic sensor was glued to the surface of the steel beam (inside the flanges) on both sides of the upper and lower flange of the 260 mm (10.236 in.) I-beam.

During the tests, the force was measured with the use of force gauges with a load-bearing capacity of up to 50 tonnes (55 tons). The beam deflection measurements were made independently using two techniques: electronic sensors and the geodetic technique. The results of deflections measured with electronic sensors and the geodetic technique were consistent.

## Ultimate limit state

Table 1 summarizes the values of loads causing the ultimate limit state  $P_{max}$  and deflections to failure  $u_{max}$  for the six continuous test beams and six simply supported test beams.

For simply supported and continuous beams, the values of loads causing the ultimate limit state were higher for beams prestressed using bonded tendons than for beams prestressed with unbonded tendons. In the simply supported beams, the average load causing the ultimate limit state was about 26% higher for beams prestressed with bonded tendons. For continuous beams, the average load causing the ultimate limit state in beams prestressed with bonded tendons was approximately 17% higher.

The values of the average deflections at the ultimate limit state were greater for simply supported beams than for continuous beams. For simply supported beams, higher deflection values (by approximately 10%) occurred at prestressing with unbonded tendons compared with bonded tendons. For continuous beams, similar deflection results were obtained for bonded and unbonded tendons. The beams failed as a result of crushing the concrete in the compression zone. Figure 5 shows an

**Table 1.** Values of loads causing the ultimate limit state  $P_{max}$  and the maximum deflection at failure  $u_{max}$

Beam	$P_{max}$ kN	$u_{max}$ mm	Beam type
1	131	46.89	Simply supported bonded tendon
4	140	41.57	
6	140	55.08	
Average	137	47.85	
9	111	54.99	Simply supported unbonded tendon
10	105	49.84	
12	110	55.19	
Average	109	53.34	
2	150	46.24	Continuous bonded tendon
3	153	42.86	
5	156	42.17	
Average	153	43.76	
7	138	41.08	Continuous unbonded tendon
8	130	45.68	
11	125	40.74	
Average	131	42.50	

Note: 1 mm = 0.0394 in.; 1 kN = 0.225 kip.

example of beam after failure. In the beams prestressed with bonded tendons, there were many cracks of considerable width at the time of failure. In the beams prestressed with unbonded tendons, one crack was visible at the time of failure and the remaining cracks that were visible after failure had a small width.

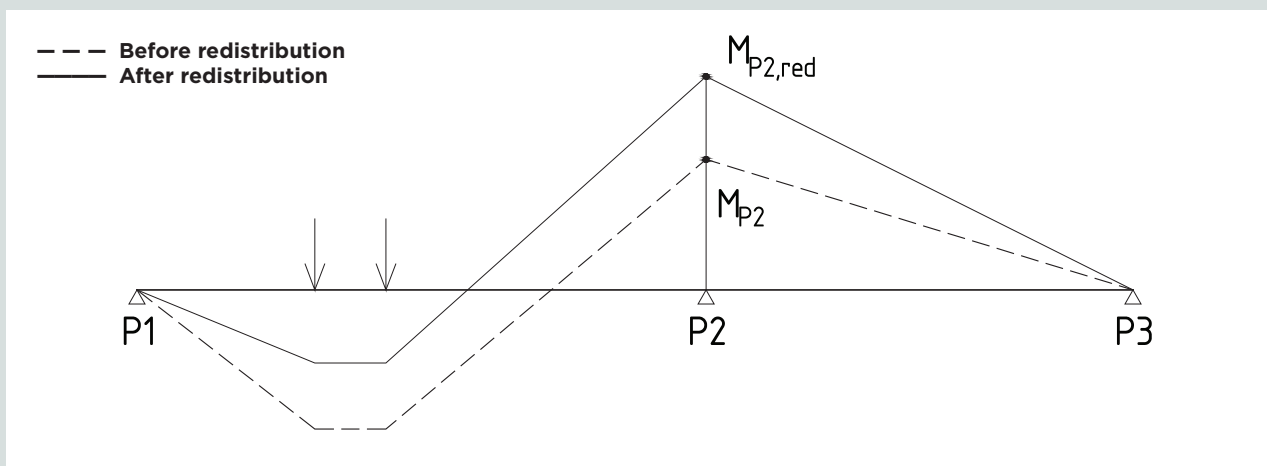


**Figure 6.** Scheme of redistribution of bending moments from span to support. Note:  $M_{p2}$  = bending moment calculated in the elastic range;  $M_{p2,red}$  = measured bending moment;  $P_1$  = extreme support;  $P_2$  = calculation point in elastic range;  $P_3$  = end support.

## Moment redistribution

The redistribution of bending moments from span to support was estimated by analyzing the tested two-span beams (Fig. 6). The degree of redistribution  $\delta$  was determined based on the analysis of change in the bending moments above the intermediate support in the steel part of the continuous beam in relation to the values calculated for the elastic range analysis. The degree of moment redistribution  $\delta(q)$  was calculated as the ratio of the measured bending moment  $M_{p2,red}$  to the bending moment calculated in the elastic range  $M_{p2}$ :

$$\delta(q) = \frac{M_{p2,red}}{M_{p2}}$$

The values of the bending moments were determined on the basis of distributed fiber-optic sensor strain measurements.

The moment redistribution coefficient  $\delta(q)$  was analyzed for successive load phases  $q$ , up to a load value of 90 kN (20.2 kip). Above this load value, the redistribution was greater than had been assumed at the design stage, and the zero point of bending moments was displaced toward the concrete part of the beam, which caused some static. The analysis of the value of the strain of the optical fibers was used to determine the change in the position of the zero point of bending

moments. Table 2 shows examples of the strain values of the optical fiber located 30 mm (1.181 in.) from the upper surface of the beam in a cross section 2500 mm (98.425 in.) away from the end support for beam 2. Initially, the optical fiber section was compressed (negative values); however, with a load of 80 kN (18 kip), it was already in the tension zone (positive values). The zero bending moment site, originally located in the area of the assembly section, shifted by more than 0.5 m (1.6 ft) due to the reduction of the stiffness of the concrete beam part, which is more than 12.5% of the length of the first span.

Tables 3 and 4 present the coefficients of moment redistribution in beams prestressed with tendons with and without bond.

For the parameter  $X$ , where  $X$  is the ratio of bending moment  $M$  to maximum moment  $M_{max}$ ,  $M$  was determined assuming a constant distribution of stiffness along the length of the beam in the elastic range and  $M_{max}$  was determined on the basis of the results obtained for simply supported beams (bending moment at the ultimate limit state). The values are given for the most stressed section in the concrete part of the beam.

For the obtained results in terms of the fixed crack pattern (after cracking), a linear function representing the change

**Table 2.** Strain values in successive load phases  $P$  in the highest section of the optical fiber in the section 2.5 m away from the extreme support  $P_1$  for continuous beam with bonded tendons (beam 2)

$P$ , kN	10	20	30	40	50	60	70	80	90	100
Strain, $\mu\epsilon$	-22	-42	-50	-49	-42	-25	-3	17	40	41

Note: 1 m = 3.281 ft; 1 kN = 0.225 kip.

**Table 3.** Coefficients of moment redistribution in beams prestressed by bonded tendons

$X = M/M_{max}$	$\delta_2$	$\delta_3$	$\delta_5$	$\delta_{avg}$
0.10	1.19	1.20	1.07	1.15
0.17	1.15	1.16	1.07	1.13
0.25	1.18	1.26	1.11	1.18
0.32	1.28	1.40	1.21	1.30
0.39	1.40	1.50	1.28	1.39
0.46	1.53	1.58	1.35	1.49
0.54	1.61	1.64	1.40	1.55
0.61	1.66	1.69	1.42	1.59
0.68	1.70	1.75	1.43	1.63

Note:  $M$  = bending moment;  $M_{max}$  = maximum moment;  $X$  = ratio of bending moment  $M$  to maximum moment  $M_{max}$ ;  $\delta_{avg}$  = average coefficient of moment redistribution for all three beams;  $\delta_2$  = beam 2 moment redistribution coefficient;  $\delta_3$  = beam 3 moment redistribution coefficient;  $\delta_5$  = beam 5 moment redistribution coefficient.

**Table 4.** Coefficients of moment redistribution in beams prestressed by unbonded tendons

$X = M/M_{max}$	$\delta_7$	$\delta_8$	$\delta_{11}$	$\delta_{avg}$
0.13	1.26	1.14	1.09	1.16
0.22	1.23	1.10	1.06	1.13
0.31	1.33	1.17	1.13	1.21
0.40	1.45	1.33	1.24	1.34
0.49	1.58	1.43	1.37	1.46
0.58	1.70	1.49	1.50	1.56
0.67	1.78	1.54	1.59	1.64
0.76	1.85	1.69	1.69	1.75
0.85	1.95	1.84	1.81	1.87

Note:  $M$  = bending moment;  $M_{max}$  = maximum moment;  $X$  = ratio of bending moment  $M$  to maximum moment  $M_{max}$ ;  $\delta_{avg}$  = average coefficient of moment redistribution for all three beams;  $\delta_7$  = beam 7 moment redistribution coefficient;  $\delta_8$  = beam 8 moment redistribution coefficient;  $\delta_{11}$  = beam 11 moment redistribution coefficient.

of the bending moment redistribution coefficient (using the fitting of points using the least squares method) was determined according to the slope-intercept equation.

$$y = mx + b$$

where

$m$  = ratio of the slope of the line to the abscissa

$x$  = the distance from the x axis

$b$  = is the point of intersection of the straight line with the ordinate axis.

The following linear equations were obtained:

- For bonded tendons,  $y = 0.79x + 1.11$ .
- For unbonded tendons,  $y = 1.11x + 0.91$ .

Based on the designated functions, the values of the coefficient of moment redistribution  $\delta$  up to the ultimate limit state exhaustion ( $M/M_{max}$  of 1.0) were extrapolated.

In the crack formation phase, beams prestressed with either bonded or unbonded tendons show similar values of the degree of moment redistribution  $\delta$  from the span to the support. With a constant pattern of cracks, a greater degree of redistribution is characteristic of beams prestressed with unbonded tendons.

The moment redistribution coefficient  $\delta$  reaches values greater than 1.0 in the elastic range. This is probably due to microcracking in the concrete that occurs in the early stages of loading. Thus, the reduction in stiffness and the associated redistribution of bending moments may likely occur before the element is visibly cracked.

Thanks to the use of modern distributed fiber-optic sensor technology, the appearance of cracks was verified during the tests on the basis of the strain of optical fibers placed in the beam (at four different points at the height of the cross section, as explained earlier). Before loading the beam with a force causing a bending moment equal to the cracking moment, local strain increases in the optical fiber sensor were observed, which indicated a probable destruction of the concrete structure and the presence of microcracks in the concrete (Fig. 7). The cracks observable on the outer surfaces of the beams appeared after reaching the value of the cracking moment. (The value of the cracking moment was determined according to Eurocode 2.<sup>1</sup>). The measuring section in Fig. 7 corresponding to the distance range from the beginning of the sensor, from 3 to 6 m (9.8 to 19.7 ft) is the lowest section of the optical fiber (50 mm [1.969 in.] from the lower surface of the beam at the height of the prestressing tendon).

The determined values of the moment redistribution coefficients were referred to as the parameter  $Y$ , where  $Y$  is the ratio of the bending moment  $M$  to cracking moment  $M_{cr}$  (Table 5 and Fig. 8). The bending moment  $M$  was determined assuming a constant distribution of stiffness along the beam length in the elastic range.

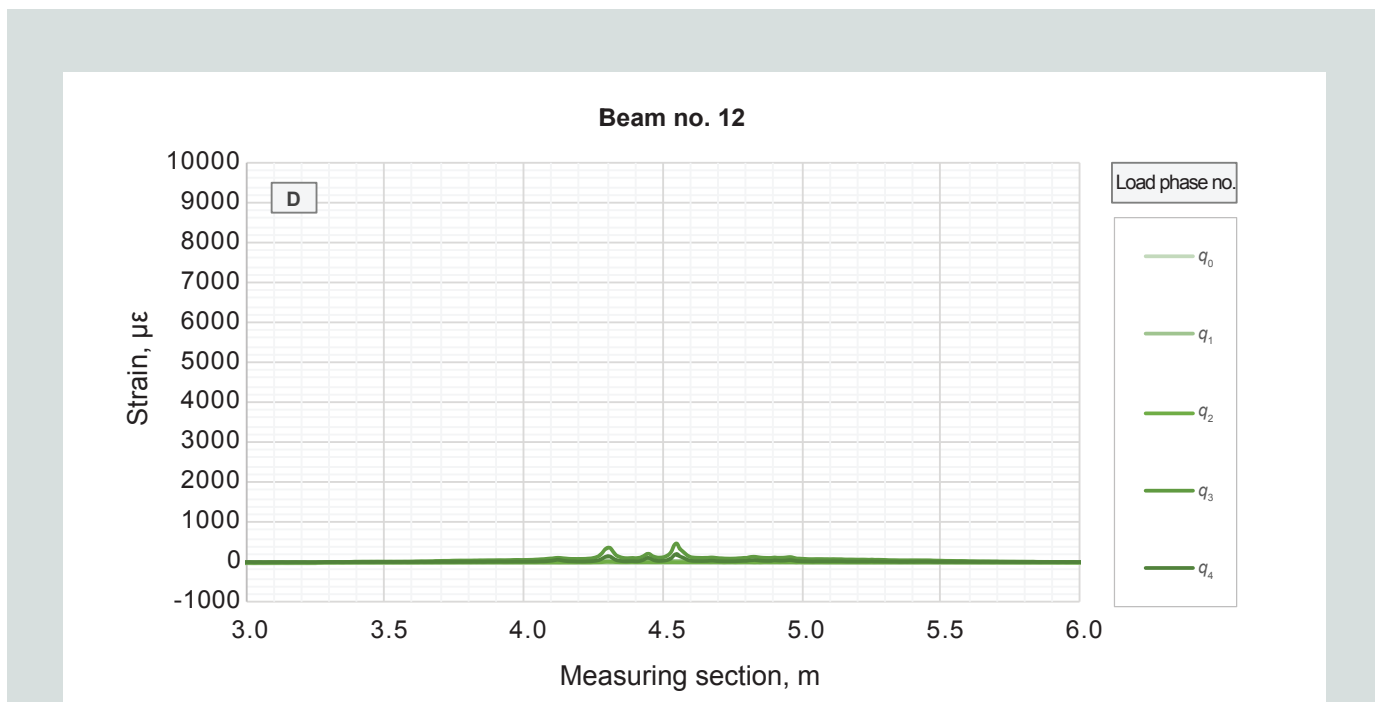


**Figure 7.** Distribution of optical fiber sensor strain in a simply supported beam with unbonded tendons (beam 12) in the initial stages of loading. Note:  $M_{cr}$  = cracking moment;  $q_0$  = load phase 0, initial measurement;  $q_1$  = load phase 1, load causing  $0.46M_{cr}$ ;  $q_2$  = load phase 2, load removal;  $q_3$  = load phase 3, load causing  $0.78M_{cr}$ ;  $q_4$  = load phase 4, load removal. 1 m = 3.281 ft.



**Table 5.** Moment redistribution coefficients in beams prestressed with bonded tendons and unbonded tendons

$Y = M/M_{cr}$	$\delta_b$	$\delta_{u/b}$
0.46	1.15	1.16
0.78	1.13	1.13
1.10	1.18	1.21
1.43	1.30	1.34
1.75	1.39	1.46
2.07	1.49	1.56
2.40	1.55	1.64
2.72	1.59	1.75
3.04	1.63	1.87

Note:  $M$  = bending moment;  $M_{cr}$  = cracking moment;  $Y$  = ratio of the bending moment  $M$  to cracking moment  $M_{cr}$ ;  $\delta_b$  = moment redistribution coefficient in beams prestressed with bonded tendons;  $\delta_{u/b}$  = moment redistribution coefficient in beams prestressed with unbonded tendons.

On the basis of the presented experimental tests, it is recommended that a finite element model be derived and validated for use in further investigation.

## Conclusion

In this experimental study, the following conclusions were made:

- A testing method using a hybrid beam structure combining prestressed concrete and steel elements proved to be successful. This is an advantageous solution because strain measurements in a steel element can be interpreted more precisely than strain measurements in a concrete element due to the constant stiffness and linear-elastic behavior of the steel element in the range of the applied loads. In the research, the measurements were made using an innovative technique using distributed fiber-optic sensor technology.
- The degree of redistribution of bending moments in continuous beams was determined. Until the value of the cracking moment was reached in the beams, the redistribution of bending moments reached up to 15%, which continued to increase almost twice until the ultimate limit state was exhausted. In the crack formation phase, beams prestressed with bonded and unbonded tendons showed similar values of the degree of redistribution of bending moments from span to support. With a constant pattern of cracks, a greater degree of redistribution was characteristic of beams compressed with unbonded tendons.
- The determined degree of moment redistribution was higher in comparison to values allowed by current codes.<sup>1</sup> It was also higher than the result of previous studies such as Kodur and Campbell.<sup>5</sup>

## Acknowledgments

The experiments were conducted at the laboratory at the University of Technology in Poznań, Poland. Special thanks go to everyone who provided help and support to complete this project.

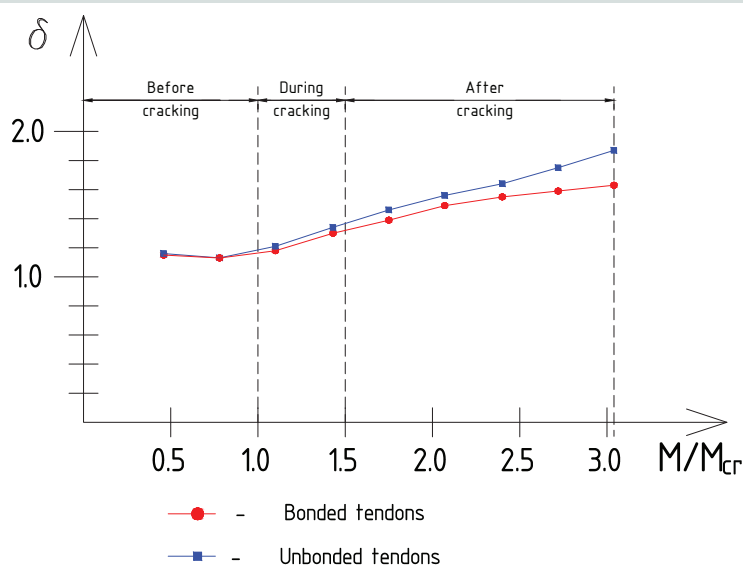


**Figure 8.** Coefficient of moment redistribution in beams prestressed with bonded tendons and unbonded tendons. Note:  $M$  = bending moment;  $M_{cr}$  = cracking moment;  $\delta$  = coefficient of moment redistribution.

## References

1. Eurocode 2: Design of Concrete Structures.
2. Lin, C.-H., and Y.-M. Chien. 2000. "Effect of Section Ductility on Moment Redistribution of Continuous Concrete Beams." *Journal of the Chinese Institute of Engineers* 23 (2): 131–141. <https://doi.org/10.1080/02533839.2000.9670531>.
3. Eibl, J. 1992. "Nichtlineare Traglastermittlung/Bestimmung." *Beton- und Stahlbetonbau* 87 (6): 137–139. <https://doi.org/10.1002/best.199200220>.
4. Jędrzejczak, M., and M. Knauff. 2008. "The Plastic Equalization Method for Bending Moments and the Rotation Capacity of Plastic Hinges in Continuous Reinforced Concrete Beams in Light of Eurocode Requirements." *Technical Sciences* 11 (2008): 108–116.
5. Kodur, V. K. R., and T. I. Campbell. 1996. "Evaluation of Moment Redistribution in a Two-Span Continuous Prestressed Concrete Beam." *ACI Structural Journal* 93 (6): 721–728. <https://doi.org/10.14359/519>.
6. Scholz, H. 1990. "Ductility, Redistribution and Hyperstatic Moments in Partially Prestressed Members." *ACI Structural Journal* 87 (3): 341–349. <https://doi.org/10.14359/2645>.
7. Pisanty, A., and P. E. Regan. 1998. "Redistribution of Moments—from Serviceability to Ultimate Limit State." *Structural Engineering International* 8 (1): 35–39. <https://doi.org/10.2749/101686698780489685>.
8. Li, L., W. Zheng, and Y. Wang. 2019. "Review of Moment Redistribution in Statically Indeterminate RC Members." *Engineering Structures* 196: 109306. <https://doi.org/10.1016/j.engstruct.2019.109306>.
9. Leung, C. C. Y., F. T. K. Au, and A. K. H. Kwan. 2013. "Non-linear Analysis and Moment Redistribution of Prestressed Concrete Members." *Engineering and Computational Mechanics* 166 (1): 9–21. <https://doi.org/10.1680/j.eacm.11.00021>.
10. Lou, T., C. Peng, T. L. Karavasilis, D. Min, and W. Sun. 2020. "Moment Redistribution versus Neutral Axis Depth in Continuous PSC Beams with External CFRP Tendons." *Engineering Structures* 209: 109927. <https://doi.org/10.1016/j.engstruct.2019.109927>.
11. Zhou, W., and W. Zheng. 2010. "Experimental Research on Plastic Design Method and Moment Redistribution in Continuous Concrete Beams Prestressed with Unbonded Tendons." *Magazine of Concrete Research* 62 (1): 51–64. <https://doi.org/10.1680/macr.2008.62.1.51>.
12. Campbell, T. I., and V. R. Kodur. 1990. "Deformation Controlled Nonlinear Analysis of Prestressed Concrete Continuous Beams." *PCI Journal* 35 (5): 42–55. <https://doi.org/10.15554/pcij.09011990.42.55>.
13. Barrias, A., J. R. Casas, and S. Villalba. 2016. "A Review of Distributed Optical Fiber Sensors for Civil Engineering Applications." *Sensors* 16 (5): 748. <https://doi.org/10.3390/s16050748>.

## Notation

$A_p$	= area of prestressing strand
$b$	= point of intersection of the straight line with the ordinate axis
$i$	= the section identifier
$m$	= ratio of the slope of the line to the abscissa
$M$	= bending moment
$M_{cr}$	= cracking moment
$M_{i,ei}$	= bending moment in section $i$ before redistribution, resulting from the analysis in the elastic range
$M_{i,red}$	= bending moment in cross section $i$ after redistribution
$M_{max}$	= maximum moment
$M_{P2}$	= bending moment calculated in the elastic range
$M_{P2,red}$	= measured bending moment
$P$	= load phase
$P_{max}$	= load causing ultimate limit state
$P_1$	= extreme support
$P_2$	= calculation point in elastic range
$P_3$	= end support
$q$	= load phase
$q_0$	= load phase 0
$q_1$	= load phase 1
$q_2$	= load phase 2
$q_3$	= load phase 3
$q_4$	= load phase 4

- $u_{max}$  = deflection to failure
- $x$  = the distance from the x axis
- $X$  = ratio of bending moment  $M$  to maximum moment  $M_{max}$
- $y$  = slope intercept
- $Y$  = ratio of the bending moment  $M$  to cracking moment  $M_{cr}$
- $\delta$  = degree of redistribution
- $\delta_{avg}$  = average coefficient of moment redistribution for all three beams
- $\delta_b$  = moment redistribution coefficient in beams pre-stressed with bonded tendons
- $\delta_{ulb}$  = moment redistribution coefficient in beams pre-stressed with unbonded tendons
- $\delta(q)$  = degree of moment redistribution
- $\delta_2$  = beam 2 moment redistribution coefficient
- $\delta_3$  = beam 3 moment redistribution coefficient
- $\delta_5$  = beam 5 moment redistribution coefficient
- $\delta_7$  = beam 7 moment redistribution coefficient
- $\delta_8$  = beam 8 moment redistribution coefficient
- $\delta_{11}$  = beam 11 moment redistribution coefficient

## About the author



Katarzyna Mossor received her BS, MSc, and PhD in civil engineering from the University of Technology in Poznań, Poland, in 2012, 2013, and 2021, respectively. Her email address is [kasia.mossor@gmail.com](mailto:kasia.mossor@gmail.com).

## Abstract

Experimental tests using an innovative hybrid concrete and steel element were conducted to define a more precise method for determining the coefficient of moment redistribution in prestressed concrete beams. Based on the test results, formulas are proposed to determine moment redistribution coefficients for beams prestressed with bonded and unbonded tendons.

## Keywords

Bonded tendons, moment redistribution, prestressed concrete, unbonded tendons.

## Review policy

This paper was reviewed in accordance with the Precast/Prestressed Concrete Institute's peer-review process. The Precast/Prestressed Concrete Institute is not responsible for statements made by authors of papers in *PCI Journal*. No payment is offered.

## Publishing details

This paper appears in *PCI Journal* (ISSN 0887-9672) V. 67, No. 6, November–December 2022, and can be found at <https://doi.org/10.15554/pcij67.6-02>. *PCI Journal* is published bimonthly by the Precast/Prestressed Concrete Institute, 8770 W. Bryn Mawr Ave., Suite 1150, Chicago, IL 60631. Copyright © 2022, Precast/Prestressed Concrete Institute.

## Reader comments

Please address any reader comments to *PCI Journal* editor-in-chief Tom Klemens at [tklemens@pci.org](mailto:tklemens@pci.org) or Precast/Prestressed Concrete Institute, c/o *PCI Journal*, 8770 W. Bryn Mawr Ave., Suite 1150, Chicago, IL 60631. 